



## STRUCTURAL ANALYSIS OF FUNCTIONALLY GRADED MATERIAL USING SIGMOADAL AND POWER LAW

Nabel Kadum ABD-ALI <sup>1</sup>, Ahmed Raee MADEH <sup>2</sup>

<sup>1</sup> Mechanical Engineering Dep., College of Engineering, University of Al-Qadisiyha, Iraq  
[nabel.abdali@qu.edu.iq](mailto:nabel.abdali@qu.edu.iq)

<sup>2</sup> College of Technical Engineering, The Islamic University, Najaf, Iraq  
Computer techniques Engineering Department  
[ahmed.raee@iunajaf.edu.com](mailto:ahmed.raee@iunajaf.edu.com)

### Abstract

The stress-strain relations, displacement distribution, stress resultants and mid plane strain resultants of a functionally graded material plate are studied using Hamilton's principle. A simply supported rectangular thick shell direct stress, inplane shear stress, transverse stress and displacement are investigated. The analysis and modeling of five layers FGM shell is carried out using MATLAB19 code with ABAQUS20 software. Using distinct materials on the top and bottom layers of the shell, a transverse uniform load in five degrees - of - freedom is applied with a specific Poisson's ratio and Young's modulus in a power and sigmoidal law function through the thickness direction. A power law was used to determine the distribution of properties through shell thickness. The results showed that the bottom layer affected significantly most stress due to subjected to the most in-plane stress while the displacement is greatest at the top layer.

Keywords: FGM shell, sigmoidal law, power law, Hamilton's principle, stress analysis.

### INTRODUCTION

Today the world is turning largely to composite materials and there is almost no use or application devoid of it due to its high performance properties that exceed or compete with materials made of steel such as resistance, stiffness, thermal insulation and corrosion in addition to light weight. The mechanical properties of the functional graded materials (FGM) differ for each material element, where the change in those properties occurs along the thickness. The power-law function, sigmoidal law function and exponential law function used to define the functions of the FGM behavior where these laws describe the variety of the top surface Young's modulus and the stress Intensification in the interfaces. The properties of main components in FGM such as thermal, mechanical, magnetic, optical are varied according to the variety of chemistry or microstructure, thus the traditional technique not useful with these components and the smooth variance in the properties of these materials results from being microscopically inhomogeneous materials [1-2]. Also, the properties of gradient materials were characterized by high performance specifications such as high bonding strength, reduced stress concentration and resistance to high thermal loads, which made these materials the focus of attention, especially in advanced and vital industries such as the manufacture of reactors, optics and electronics,

in addition to the uses of mechanical and medical engineering [3].

In engineering applications that are exposed to impact loads in addition to thermal loads, engineering structures must provide sufficient support to withstand those loads, making the observations directed towards specific materials that have the ability to withstand those loads together [4-5]. The advantage of the mixture of ceramic with low thermal conductivity, and other materials or a combination of other metals to improve the capability to withstand high-temperature gradient environments in addition to keeping their structural strength Also, the possibility of manufacturing these mixtures with a constantly varying volume fraction [6].

The integral form from the Refined Zigzag Theory (RZT) equilibrium equations by Peridynamic Differential Operator (PDDO) to achieve the perfect solution of the differential equations and considered this theory is more appropriate for thick as well as moderately thick plate stress analysis due to independent on the correction factors of shear and involve several of kinematic variables. The stress concentration was reducing at the interface core as well as face sheet due to use the functionally graded cores [7].

The nonlinear vibration of nanotube composite with single-walled functionally graded beam by nonlinear von Kármán geometric and theory of Timoshenko beam were discussed by other researchers [8] and the static and modal analysis

were described for simply supported conditions of plate with function graded properties across thickness as well as volume fraction variance [9]. Specific studies reported the graduation of material properties in transverse and axially thickness direction according to power law to study the characteristic of dynamic analysis. A virtual work principle was used to derive the equation of motion and the model discretization was treated by finite element method [10]. Also, the axial stress analysis which effected by various types of functionally graded beam was evaluated under thermal environment [11].

The excellent properties of FGM as well as corrosion and erosion resistant in addition to thermal characteristics prompted researchers to study the use these components in free and force buckling analysis under different thermal effect [12]. A plate with a novel functionally graded with smoothly distribution of stress through the thickness to avoid interfacial failure of sandwich plate structure was discussed and the mechanical properties such as shear modules and Poisson's ratio were varied through thickness. the equations of motion were solved by using Ritz method with Chebyshev polynomials to obtain bending deflection, shear buckling load and stresses for simply supported and clamped plate [13]. Also, the NURBS functions were used to describe the displacement of element that depends on parameters of function graded material and the stiffness of the thick plate including extension-bending coupling [14].

Other studies evaluate nonlinear eigenvalue analysis of FGM nanocomposite with carbon nanotube as reinforcement agent with different distribution in direction of thickness depend on beam theory of Timoshenko and nonlinear theory of Karman, where the volume fraction, slenderness ratio and amplitude of vibration were discussed through free vibration state [15]. Other studies described the sigmoid-law in distribution of different material properties such as ceramic and metal through thickness of beam. Stiffness and buckling matrices were built by the finite element model and solved free vibration analysis numerically [16]. In addition, other researches investigate the dynamic response of functionally graded for axi-symmetric plate and cylinders under thermo-mechanical and finite element formulation under thermal load using theory of first order shear (FSDT) [17].

Present work focus on the mechanical properties of multilayer composite material, where The stress-strain relations strain displacement, stress resultants and mid plane strain resultants of a functionally graded material plate are studied using Hamilton's principle. A simply supported rectangular shell direct stress, inplane shear stress, transverse stress and displacement are investigated.

## MATHEMATICAL FORMULATION

A distinctive material properties  $P$  is differed through the thickness of plate along the expressions of the power law [18]:

$$P(z) = (P_t - P_b)V + P_b, \quad V = \left(\frac{z}{h} + \frac{1}{2}\right)^n \quad (1)$$

where  $P_t$  and  $P_b$  refer to the top and bottom plate faces property, respectively, and parameter  $n$  indicates the profile variation of the material along the thickness where at fully ceramic plate, the value of  $n$  equal to zero. Stress concentrations arise on one of the interfaces in which the material is continuous but varies rapidly when a FGM of a single power-law function is applied to the multi-layered laminated shell. To achieve a smooth distribution of stresses across all interfaces, the volume fraction was determined using two power-law functions.

A transverse force is applied to a linearly elastic, medium-thick, rectangular FGM shell. The thickness  $h$  of a medium-thick FGM shell is considered to be uniform, and the thickness  $h$  is in the range of  $1/20$   $1/100$  of its span.

1. Before and after deformation, line segments perpendicular to the middle surface remain unstretched and normal.
2. The FGM shell deflections are small in compared to its thickness  $h$ , therefore linear strain-displacement relationships are acceptable.
3. Because the thickness is considered to be in the range of  $1/20$   $1/100$  of its span, the normal stress in the thickness direction may be ignored.
4. The Young's modulus and Poisson's ratio of the non-homogeneous elastic FGM are functions of the spatial coordinate  $z$ .

The FGM plate's deformations and stresses are based on the following assumptions:

The principal equations of motion and the models of finite element developed for the classical plate theory and First- order theory are suitable for the multi-layers plates. The stiffness of plate were devoted by [19]:

$$(A_{ij}, B_{ij}, D_{ij}) = \int_{-\frac{h}{2}}^{\frac{h}{2}} Q_{ij}(z) (1, z, z^2) dz \quad (i, j = 1, 2, 6) \quad (2)$$

$$A_{ij} = \int_{-\frac{h}{2}}^{\frac{h}{2}} Q_{ij}(z) dz \quad (i, j = 4, 5) \quad (3)$$

$$(I_0, I_1, I_2) = \int_{-\frac{h}{2}}^{\frac{h}{2}} \left[ (\rho_c - \rho_m) \left( \frac{2z+h}{2h} \right) + \rho_m \right] (1, z, z^2) dz \quad (i, j = 1, 2, 6) \quad (4)$$

$$Q_{11} = Q_{22} = \frac{E(z)}{1-\nu^2} \quad (5)$$

$$Q_{12} = Q_{21} = \frac{\nu E(z)}{1-\nu^2} \quad (6)$$

$$Q_{44} = Q_{55} = Q_{66} = \frac{E(z)}{2(1+\nu)} \quad (7)$$

where the subscripts, c and m refer to the ceramic and metal, respectively, while the coefficient of thermal expansion and the modulus as well as the coefficients of elastic  $Q_{ij}$  differ through the thickness of plate. [8]

Also, the strain and kinetic energies may be stated respectively as [20]:

$$U_e = \iiint \sigma_{ij} \varepsilon_{ij} \delta \, dx \, dy \, dz \quad (8)$$

$$T_e = \frac{1}{2} \iint \rho \, h \, w^2 \, dx \, dy \quad (9)$$

The four position for each element have 3DOF where the transverse displacement represented by w as well as  $\theta_x, \theta_y$  act x and y axis rotations respectively [21].

The matrices of stiffness and mass elements were developed on the minimum potential and kinetic energy principle [8]:

$$[K_e] = \int [B]^T [D] [B] \, dv \quad (10)$$

Where

$$[B]^T = z \begin{bmatrix} \frac{\partial^2}{\partial x^2} & \frac{\partial^2}{\partial y^2} & 2 \frac{\partial^2}{\partial x \partial y} \end{bmatrix} [N]^T \quad (11)$$

and

$$[M_e] = \int [N]^T [\rho] [N] \, dv \quad (12)$$

The Hamilton's principle was used to obtain the equation of motion for plate [22]:

$$\int_{t_1}^{t_2} (U_e - T_e + W_e) \, dt = 0 \quad (13)$$

The constitutive law, also known as the generalized law of Hooke, establishes the desired connection by using the concept of linear elastic material behaviour [22].

$$\sigma = C \varepsilon \quad (14)$$

The stresses and strains are linearly linked in this case thanks to the constitutive matrix C. Taking use of symmetry and taking strain energy into account. As demonstrated in equation (15), the anisotropic materials may be described using just 21 constants [28].

$$\begin{Bmatrix} \sigma_x \\ \sigma_y \\ \sigma_z \\ \tau_{xy} \\ \tau_{yz} \\ \tau_{xz} \end{Bmatrix} = \begin{bmatrix} C_{11} & C_{12} & C_{13} & C_{14} & C_{15} & C_{16} \\ C_{21} & C_{22} & C_{23} & C_{24} & C_{25} & C_{26} \\ C_{31} & C_{32} & C_{33} & C_{34} & C_{35} & C_{36} \\ C_{41} & C_{42} & C_{43} & C_{44} & C_{45} & C_{46} \\ C_{51} & C_{52} & C_{53} & C_{54} & C_{55} & C_{56} \\ C_{61} & C_{62} & C_{63} & C_{64} & C_{65} & C_{66} \end{bmatrix} \begin{Bmatrix} \varepsilon_x \\ \varepsilon_y \\ \varepsilon_z \\ \gamma_{xy} \\ \gamma_{yz} \\ \gamma_{xz} \end{Bmatrix} \quad (15)$$

As explained in the basic material coordination system, the constitutive relation of orthotropic materials is simplified:

$$\begin{Bmatrix} \sigma_1 \\ \sigma_2 \\ \sigma_3 \\ \tau_{12} \\ \tau_{23} \\ \tau_{13} \end{Bmatrix} = \begin{bmatrix} Q_{11} & Q_{12} & 0_{13} & 0_{14} & 0_{15} & 0_{16} \\ Q_{21} & Q_{22} & 0_{23} & 0_{24} & 0_{25} & 0_{26} \\ 0_{31} & 0_{32} & Q_{33} & 0_{34} & 0_{35} & 0_{36} \\ 0_{41} & 0_{42} & 0_{43} & Q_{44} & 0_{45} & 0_{46} \\ 0_{51} & 0_{52} & 0_{53} & 0_{54} & Q_{55} & 0_{56} \\ 0_{61} & 0_{62} & 0_{63} & 0_{64} & 0_{65} & Q_{66} \end{bmatrix} \begin{Bmatrix} \varepsilon_1 \\ \varepsilon_2 \\ \varepsilon_3 \\ \gamma_{12} \\ \gamma_{23} \\ \gamma_{13} \end{Bmatrix} \quad (16)$$

In terms of engineering constants, the constants Q can be described by [29]:

$$\left. \begin{aligned} Q_{11} &= \frac{E_1(Z)}{\psi}, & Q_{12} &= \frac{E_1(Z)\nu_{21}}{\psi} \\ Q_{21} &= \frac{E_2(Z)\nu_{12}}{\psi}, & Q_{22} &= \frac{E_2(Z)}{\psi} \\ Q_{33} &= E_3(Z) \\ Q_{44} &= G_{12}, & Q_{55} &= \gamma G_{23}, & Q_{66} &= \gamma G_{13} \end{aligned} \right\} \quad (17)$$

Where  $\psi = 1 - \nu_{12}\nu_{21}$

### Finite Element Modeling Technique

A functionally graded material is a new technology used to create composite material that may be developed for use in high temperature layer and heat shield applications due to its superior mechanical and thermal characteristics.

The FGM properties will be change during the thickness and the numerical model consist of various layers in order to get this variation in properties as shown in the figures (1), (2) and (3). From the bottom surface, the material properties are evaluated with using the different laws of volume fraction distribution. Even though, the layered of structure does not show the material properties gradation, a adequate layers number can practically approximate the gradation of material peoperties. In this work, the analysis and modeling of FGM shell is carried out using ABAQUS software. ABAQUS proposes a more elements to select from for the gradient materials in the modeling. The FGM properties subjected to mechanical loads examined on a flat shell.

Ply Name	Region	Material	Thickness	CSYS
1	(Picked)	AL2O3	0.002	<Layup>
2	(Picked)	GF 0/90	0.005	<Layup>
3	(Picked)	CF 0	0.003	<Layup>
4	(Picked)	GF 0/90	0.005	<Layup>
5	(Picked)	GF 0	0.003	<Layup>

Fig. 1. Layers material properties

Material	Thickness	Orientation Angle	Integration Points	Ply Name
AL2O3	0.002	0	3	1
GF 0/90	0.005	0/90	3	2
CF 0	0.003	0	3	3
GF 0/90	0.005	0/90	3	4
GF 0	0.003	0	3	5

Fig. 2. Layers material type with orientation angles

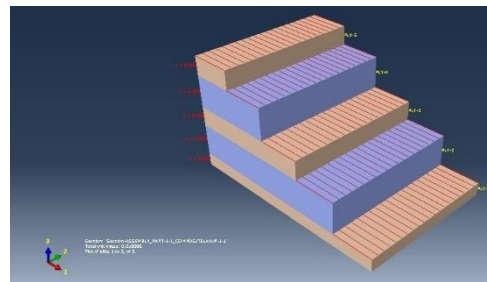


Fig. 3. Distribution of thickness and properties in each layer

Take into consideration a symmetrically, rectangular laminated thick shell with simply supported edges boundary conditions as shown in Fig. 4 and subjected to an uninformed pressure. Transverse shear deformations are taken into consideration, which may be essential if the shell is thick or involves layers with a low transverse shear modulus. The thick shell can be laminated cross-ply (symmetric or anti-symmetric) as well as angle-ply symmetrically with a large number of layers, or orthotropically.

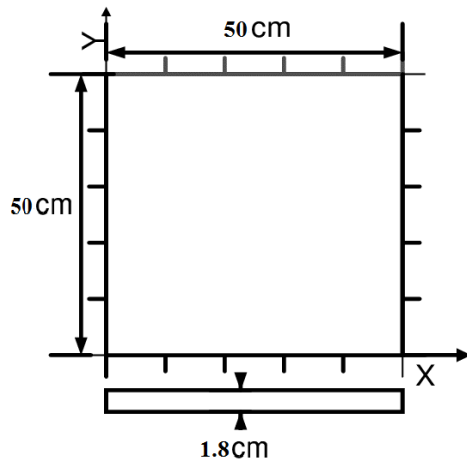


Fig. 4. Simply supported rectangular shell

### Results and Discussions

Stress concentrations arise on one of the interfaces where the material is continuous but varies significantly when a FGM of a single power-law function is applied to the multi-layered composite. To achieve a smooth distribution of stresses across all interfaces, the volume fraction was determined using two power-law functions. Consider an elastic rectangular plate and shell. The local coordinates  $x$  and  $y$  defined at the thick shell's edge, but the  $z$ -axis, which began at the shell's center surface, is really in the thickness direction. The top and lower surfaces have distinct material characteristics, such as Young's modulus and Poisson's ratio, also they are pre-defined based on the performance requirements. The Young's modulus and Poisson's ratio of the plates and shells, on the other hand, only vary uniformly in the thickness direction ( $z$ -axis), resulting in the following: Plate and shell made of functionally graded material (FGM).

The two power law functions are illustrated in the figures (5) and (6).

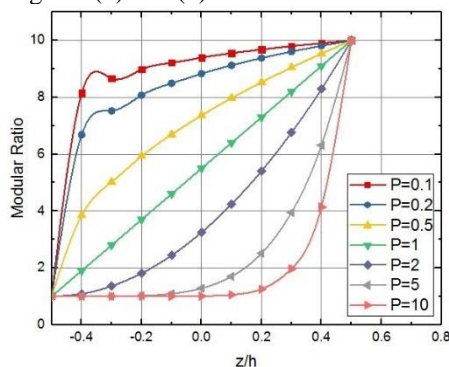


Fig. 5. The variation of Modular ratio in a P-FGM shell

The change of Modular ratio with sigmoid distributions is shown in Fig. 6, and this FGM shell is hence known as a sigmoid FGM shell (S-FGM). The stiffness of the S-FGM of thick shell reduces as the power law index increases, whereas the load vector increases as the variational parameter increases. The magnitude of deflection increases as the value of the power law index increases, and the

magnitude of deflection increases as the value of the variational parameter increases.

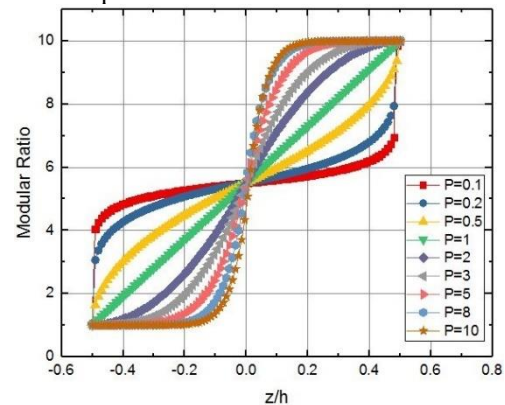


Fig. 6. The variation of Modular ratio in a S-FGM shell

### Static Analysis

The numerical results for the combined large deflection of a simply supported functionally graded square shell in the figure (7) exposed to uniformly distributed pressure were provided in the static analysis, as illustrated in figure (8). The intensity of deflection increases as the power law index increases. The influence of transverse shear deformation may be to increase deflection, as predicted. When the thickness ratio is small, the differences in deflection values predicted by the current model are significant, but they become trivial as the side-to-thickness ratio increases.

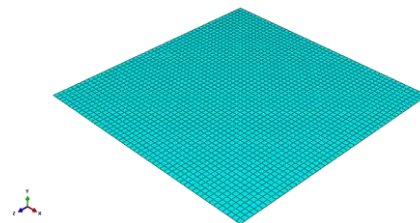


Fig. 7. Element of meshing shell

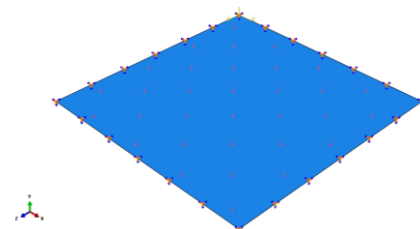


Fig. 8. Pressure distribution with boundary conditions

The translation and rotation displacements through the thickness at the shell center are shown in figures (9) and (10). The geometrical parameters and material properties used are defined in figure (1), with aluminum oxide for the bottom and top surfaces. Using a uniform mesh, model only one quadrant of the domain, taking use of the biaxial symmetry.

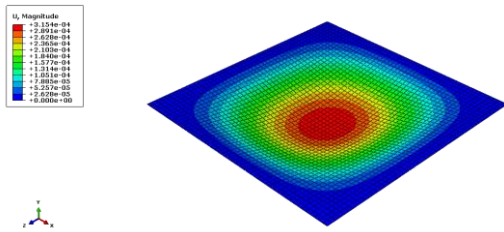


Fig. 9: Translation displacement distribution

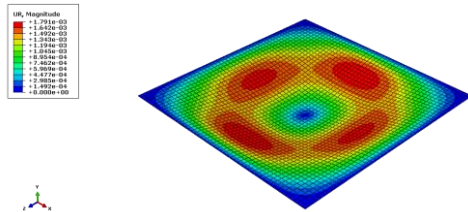


Fig. 10: Rotation displacement distribution

The stress coefficient in the z direction is 0 since the load was applied transversely. The magnitude of the stress coefficients in the x and y directions was determined to be the same. Shear stress was also determined to have the same magnitude in the xz and yz planes.

Figures (11) and (12) shows the distribution of maximum Von Mises and Tresca stress distribution. The maximum value of stress was found at the edge support due to the Von Mises stress was related to the bending moment which become maximum at this supports. There is a high level of agreement between the current and published results. The results demonstrate that the current formulation performs exceptionally well in terms of accuracy.

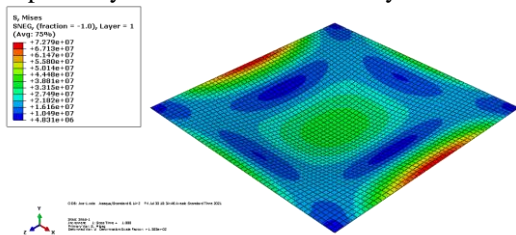


Fig. 11: Von Mises stress distribution

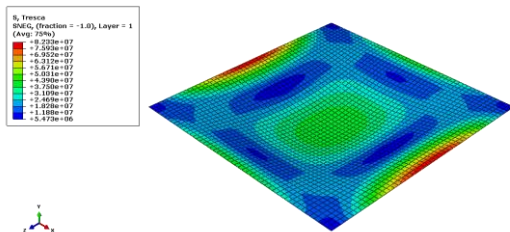


Fig. 12: Tresca stress distribution

Figures (13), (14) and (15) show the variation of tensile stress ( $\sigma_x$ ), ( $\sigma_y$ ) and shear stress ( $\sigma_{xy}$ ) respectively for specified boundary conditions of a square shell with uniformly distributed load for P-GM. From the extracted result of distribution, the

variation of stress can be noted in the direction of stress coordinate for ( $\sigma_x$ ) and ( $\sigma_y$ ) and in the shear direction for the ( $\sigma_{xy}$ ).

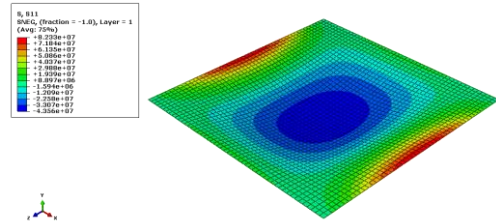


Fig. 13: Tensile stress ( $\sigma_x$ ) distribution

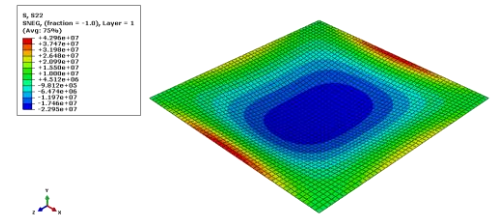


Fig. 14: Tensile stress ( $\sigma_y$ ) distribution

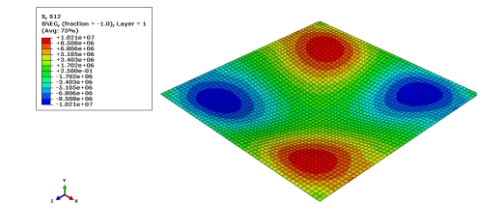


Fig. 15: Shear stress ( $\sigma_{xy}$ ) distribution

Figures (16), (17) and (18) illustrate the change of strain distribution in (x) and (y) direction as well as shear strain (xy) for stated boundary conditions of a square shell under uniformly distributed load. The fluctuation of strain in the direction of strain coordinate for (x) and (y) and in the shear direction for (xy) may be observed from the extracted result of distribution.

Strain distribution is related to the strain energy, also called as deformation energy, is the potential energy contained in an object as strain and stress. The work done by the external force is transformed into energy stored in the solid throughout deformation process, which is known as elastic strain energy. The stored energy is known as deformation energy or strain energy when it is acted upon by an external force. Elastic deformation energy and plastic deformation energy are two types of deformation energy. The solid will release part of its energy and work when the external force and deformation are gradually reduced, and this part of the energy is elastic deformation energy.

Several works were focused on manufacturing process of composite materials with different properties and different engineering applications to investigate the mechanical behavior of these components and to improve its properties [23-27]. The present study looks forward to use new

reinforcement materials with new layer arrangement to improve specific applications.

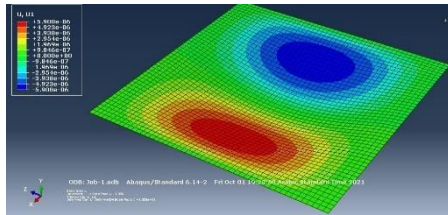


Fig. 16. Shear strain ( $\epsilon_{xy}$ ) distribution

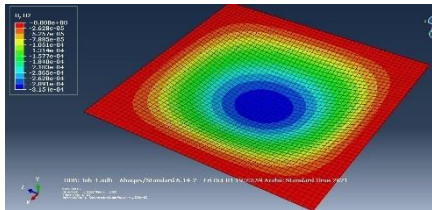


Fig. 17. Shear strain ( $\epsilon_{xy}$ ) distribution

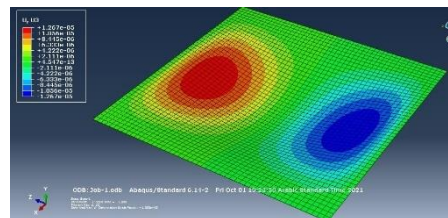


Fig. 18. Shear strain ( $\epsilon_{xy}$ ) distribution

## CONCLUSIONS

Some conclusions may be extracted from this work such as:

1. When a transverse load is supplied to a FGM, a bottom section of the shell receives significantly more stress than the top portion; consequently, it really is important to build the FGM with a high Young's modulus at the bottom to avoid fracture.
2. Mostly in case of in-plane stress, the part at the top is subjected to the most in-plane stress. In the FGM, the displacement is greatest at the top particle.
3. The sigmoidal law produces excellent results for the quality and improve of stresses. Both the theoretical equations and the FEM model provided significant and acceptable results for bending stress and bending strain.
4. Power law give smooth or uniform stress distribution through the thickness and can be used for high stress applications.
5. The maximum deformation capacity that satisfies the practicability is determined to achieve the maximum bearing capacity, based on the amount of deformation and stress energy of the shell.

## REFERENCES

1. Ramu I, Mohanty SC. Modal analysis of functionally graded material plates using finite element method. *Procedia Materials Science*. 2014; 6:460-467.
2. Bobbio LD, Otis RA, Borgonia JP, Dillon RP, Shapiro AA, Liu ZK, Beese AM. Additive manufacturing of a functionally graded material from Ti-6Al-4V to Invar: Experimental characterization and thermodynamic calculations. *Acta Materialia*. 2017; 127:133-142. <https://doi.org/10.1016/j.actamat.2016.12.070>
3. Yamanouchi M, Koizumi M, Hirai T, Shiota I. Proc. First Int. Sympos. Functionally Gradient Materials. Japan, 1990.
4. Koizumi M. The concept of FGM, ceramic trans. *Functionally Gradient Materials*. 1993; 34.3-10.
5. Eltaher MA, Alshorbagy AE, Mahmoud FF. Determination of neutral axis position and its effect on natural frequencies of functionally graded macro/nanobeams. *Composite Structures*. 2013;99: 193-201. <https://doi.org/10.1016/j.compstruct.2012.11.039>.
6. Yin HM, Sun LZ, Paulino GH. Micromechanics-based elastic model for functionally graded materials with particle interactions. *Acta Materialia*. 2004;52(12): 3535-3543.
7. Chi SH, Chung YL. Mechanical behavior of functionally graded material plates under transverse load-Part I: Analysis. *International Journal of Solids and Structures*. 2006;43(13): 3657-3674.
8. Reddy JN, Chin CD. Thermomechanical analysis of functionally graded cylinders and plates. *Journal of thermal stresses*. 1998;21(6):593-626. <https://doi.org/10.1080/01495739808956165>
9. Dorduncu M. Stress analysis of sandwich plates with functionally graded cores using peridynamic differential operator and refined zigzag theory. *Thin-Walled Structures*. 2020;146:106468. <https://doi.org/10.1016/j.tws.2019.106468>
10. Ke LL, Yang J, Kitipornchai S. Nonlinear free vibration of functionally graded carbon nanotube-reinforced composite beams. *Composite Structures*. 2010;92(3):676-683. <https://doi.org/10.1016/j.compstruct.2009.09.024>
11. Burlayenko VN, Sadowski T. Free vibrations and static analysis of functionally graded sandwich plates with three-dimensional finite elements. *Meccanica*. 2020;55(4):815-832. <https://doi.org/10.1007/s11012-019-01001-7>
12. Alshorbagy AE, Eltaher MA, Mahmoud FF. Free vibration characteristics of a functionally graded beam by finite element method. *Applied Mathematical Modelling*. 2011;35(1):412-425. <https://doi.org/10.1016/j.apm.2010.07.006>
13. Boğa C, Selek O. Stress Analysis of Functionally Graded Beams Due to Thermal Loading. *Journal of Engineering Science and Technology*. 2020;15(1): 054-065.
14. Pradhan P, Sutar MK, Pattnaik S. A state of the art in functionally graded materials and their analysis. *Materials Today: Proceedings*. 2019;18:3931-3936. <https://doi.org/10.1016/j.matpr.2019.07.333>.

15. Chen D, Yang J, Kitipornchai S. Buckling and bending analyses of a novel functionally graded porous plate using Chebyshev-Ritz method. *Archives of Civil and Mechanical Engineering*. 2019;19(1):157-170. <https://doi.org/10.1016/j.acme.2018.09.004>.
16. Gilewski W, Pelczyński J. Material-oriented shape functions for FGM plate finite element formulation. *Materials*. 2020;13(3):803. <https://doi.org/10.3390/ma13030803>
17. Afshin A, Nejad MZ, Dastani K. Transient thermoelastic analysis of FGM rotating thick cylindrical pressure vessels under arbitrary boundary and initial conditions. *Journal of Computational Applied Mechanics*. 2017;48(1):15-26. <https://doi.org/10.22059/jcamech.2017.233643.144>.
18. Benyamina AB, Boudierba B, Saoula A. Bending response of composite material plates with specific properties, case of a typical FGM “ceramic/metal” in thermal environments. *Periodica Polytechnica Civil Engineering*. 2018;62(4):930-938.
19. Chen Y, Jin G, Zhang C, Ye T, Xue Y. Thermal vibration of FGM beams with general boundary conditions using a higher-order shear deformation theory. *Composites Part B: Engineering*. 2018;153: 376-386. <https://doi.org/10.1016/j.compositesb.2018.08.111>.
20. El-Megharbel A. A theoretical analysis of functionally graded beam under thermal loading. *World Journal of Engineering and Technology*. 2016; 4(3):437-449. <https://doi.org/10.4236/wjet.2016.43044>.
21. Evran S. Bending stress analysis of axially layered functionally graded beams. *Ömer Halisdemir Üniversitesi Mühendislik Bilimleri Dergisi*. 2018; 7(1):390-398. <https://doi.org/10.28948/ngumuh.387230>
22. Ashrafi HR, Beiranvand P, Aghaei MZ, Jalili DD. Modal Analysis of FGM Plates (Sus304/Al2O3) Using FEM. *Bioceram Dev Appl*, 2018;8(112):2. <https://doi.org/10.4172/2090-5025.1000112>.
23. Abd-Ali NK, Farhan MM, Hassan NY. Improvement of mechanical properties of the rubbery part in cement packing system using new rubber materials. *Journal of Engineering Science and Technology*. 2021; 16(2): 1601–1613.
24. Abd-Ali NK, The effect of cure activator zinc oxide nanoparticles on the mechanical behavior of polyisoprene rubber. *Journal of Engineering Science and Technology*. 2020;15(3):2051–2061.
25. Abd-Ali NK, Madeh AR, Experimental and numerical investigation of factors that affecting in frictional welding of mild steel and Al alloy A356, ICOASE 2018 - International Conference on Advanced Science and Engineering. 2018:456–461.
26. Ali NKA. A new reinforcement material for rubber compounds (Sediment dust nanoparticles and white cement). 1st International Scientific Conference of Engineering Sciences - 3rd Scientific Conference of Engineering Science, ISCES 2018 – Proceedings. 2018:163–168.
27. Farhan MM, Abd-Ali NK, Hassan NY. Development the performance of the rubbery discharge part in flexo-pump system. *Journal of Engineering and Applied Sciences*. 2018;13(24):10148–10157
28. Madeh AR, Majeed WI. Effect of boundary conditions on thermal buckling of laminated composite shallow shell. *Materials Today: Proceedings*. 2021;42:2397-2404. <https://doi.org/10.1016/j.matpr.2020.12.501>
29. Fatoni NF, Park WR, Kwon OH. Mechanical property evaluation of functionally graded materials using two-scale modeling. *Journal of the Korean Society of Marine Engineering*. 2017;41(5):431-438.

Received 2021-04-18

Accepted 2021-11-23

Available online 2021-11-24



**Prof. Dr. Nabel Kadum Abd-Ali**, received his PhD degree in applied mechanics in 2013 from the University of Technology/Baghdad. He is a teacher in the department of Mechanical engineering in the University of Al-Qadisiyah, Iraq. Research topics: composite materials, rubber technology, polymer engineering, mechanical behaviour of materials.



**Ahmed Raee Madeh**, PhD student in Applied Mechanics at university of Baghdad, Formal lecturer in computer Engineering Techniques, The Islamic university, Iraq, Research topics: Vibration, stress analysis, Analytical solution.